Engineering 9 (2022) 95–100

Contents lists available at ScienceDirect

Engineering

journal homepage: www.elsevier.com/locate/eng

Research
Polymer Engineering—Article

Industrial-Scale Polypropylene–Polyethylene Physical Alloying Toward Recycling

Jinping Qu *,#, Zhaoxia Huang #, Zhitao Yang #, Guizhen Zhang, Xiaochun Yin, Yanhong Feng, Hezhi He, Gang Jin, Ting Wu, Guangjian He, Xianwu Cao

National Engineering Research Center of Novel Equipment for Polymer Processing & Key Laboratory of Polymer Processing Engineering of the Ministry of Education & Guangdong Key Laboratory of Technique and Equipment for Macromolecular Advanced Manufacturing, School of Mechanical and Automotive Engineering, South China University of Technology, Guangzhou 510640, China

ARTICLE INFO

Article history:
Received 10 July 2020
Revised 24 August 2020
Accepted 6 February 2021
Available online 14 August 2021

Keywords:
Polypropylene
Polyethylene
Physical alloying
Honeycomb structure

ABSTRACT

Polypropylene (PP) and polyethylene (PE) play central roles in our daily life. However, their immiscibility presents a major hurdle in both industry and academia when recycling them into alloys with favorable mechanical properties. Moreover, typical compatibilizer-enabled approaches are limited due to increased environmental concerns. Herein, inspired by a traditional Chinese technique, we report a facile, industry-scale methodology that produces a PP/PE binary blend with a highly ordered honeycomb nanostructure without any additives. Due to its nanostructure, the blend exhibits enhanced tensile properties in comparison with the parent components or with a sample prepared using an internal mixer. This approach has potential for applications not only in immiscible polymer blending, but also in non-sorting, compatibilizer-free waste plastics recycling. Through this technique, we expect that an environmentally friendly and sustainable plastic wastes recycling avenue can be found, and great economic benefits can be gained.

1. Introduction

Plastics have greatly facilitated our modern lifestyle by offering high performance at a relatively low price, along with low density and easy processing, since their first wide-spread use during World War II. Recently, however, the situation has changed. Rather than being considered as a potential replacement for metal-based materials, the once valuable plastics are now regarded as plastic pollution due to their long-term chemical stability, which results in serious post-treatment issues. More specifically, several influential organizations have raised concerns about plastic pollution in the seas and oceans, highlighting the challenge of plastic wastes treatment. For example, due to their potential for residual harm to the environment and to human health, plastic cutlery and packages are prohibited in Hainan, China, as of 2020.

Although several approaches have been investigated to reduce the use of plastics in order to solve the issue of plastic pollution, they have proven to be ineffective. Furthermore, such methods cannot solve the problem of pollution from plastics that have already been manufactured and are now currently in use. As reported [1], the current amount of plastic waste without appropriate treatment is as high as 5700 million metric tons globally, resulting in a serious environmental disaster. Thus, how to deal with such an enormous amount of plastic waste is a key question in both academia and industry.

The recycling of plastic waste currently attracts a great deal of attention due to its potential for completely resolving this global environmental issue. However, the accompanying long-standing challenge of making immiscible polymer blends compatible presents a roadblock in this endeavor. For example, among plastics, polypropylene (PP) and polyethylene (PE) have the highest levels of production and usage [2]; thus, the high-value recycling of their wastes is a top priority for industries. Although PP and PE have similar chemical structures, the differences in their molecular weights, molecular weight distributions, and crystal structures result in serious phase separation and poor mechanical properties when the two are combined. Many efforts have been made to circumvent the immiscibility of these two polymers in order to combine them into high-performance materials with favorable interfacial properties. However, thus far, the state-of-the-art

* Corresponding author.
E-mail address: jpqu@scut.edu.cn (J. Qu).
# These authors contributed equally to this work.

https://doi.org/10.1016/j.eng.2021.02.021

approaches in recycling PP and PE blends involve either sorting or compounding them with additives [3].

Although sorting plastic wastes into their individual polymeric components is widely done in industry, it has unfortunately been proven to be both cost prohibitive and inefficient [4]. Among all the techniques that have been developed [5–7] to circumvent this economically prohibitive and sometimes impossible process, compounding multicomponent wastes with several additives is considered to be a promising route for waste plastics recycling. Significant progress has been made in synthesizing various additives to combine PP and PE [3,4]. More specifically, the development of PP/PE multiblock copolymers has resulted in PP/PE alloys with outstanding mechanical properties [2]. Despite these advancements, the high cost and potential toxicity of these additives—as well as their low lab-scale efficiencies—still block the pathway to industrial-scale waste plastics recycling. Thus, the development of a highly efficient and eco-friendly approach for high-value PP/PE alloys remains challenging. Moreover, according to the current understanding of compatibilizing immiscible polymers, chemicals are always necessary. However, when considering both industrial availability and environmental capacity, a physical technique for fabricating PP/PE alloys is more favorable than a chemical technique.

To deal with this problem, we aimed to gain inspiration from the ancients. Yingxing Song, a famous scientific pioneer in China's Ming dynasty, wrote a book that reviewed several traditional daily used techniques [8]. In his book, Song described a traditional technique that involved applying a cycled transient pressure on soy in order to continuously generate soybean oil. Following this methodology, we considered how such a cycled transient pressure could be used in polymer blending. Herein, we use PP and PE as models to investigate the effect of cycled transient pressure. A novel technique, named industrial-scale transient stress processing (ISTSP), in which an in-house-made eccentric rotor extruder (ERE) generates cycled transient pressure, is used to realize PP/PE physical alloying without any additives, as shown in Fig. 1. A detailed description of the ERE is given in the Fig. S1 in Appendix A.

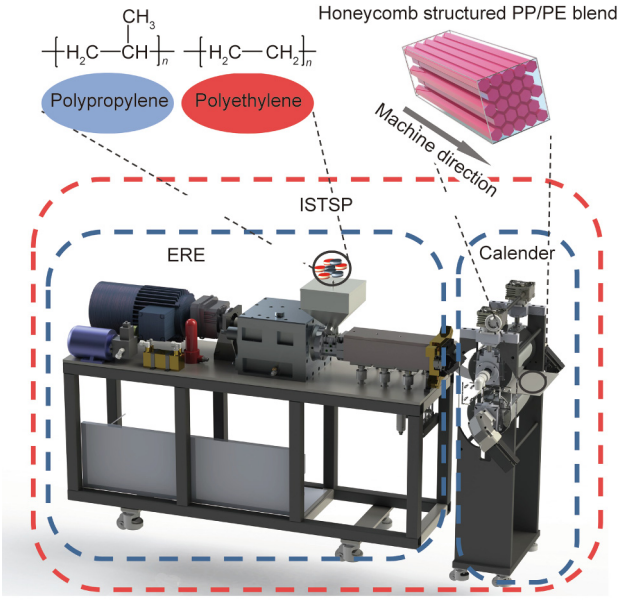

Fig. 1. Schematic of ISTSP PP/PE alloy fabrication. During the remanufacturing, bulk PP and PE were fed into the ERE after being pre-blended with a constant composition. The extrudate was then calendered into a plate shape.

2. Experimental procedure

2.1. Materials

Bulk PP with the trade name FC801 (Sinopec, China) is a homopolymer with a melt flow index (MFI) of 8.0 g per10 minutes (2.16 kg at 230 °C, ASTM D-1238). Bulk PE was used with the trade name HMA-025 (Exxon Mobil, Germany), which has an MFI of 8.2 g per 10 minutes (2.16 kg at 190 °C, ASTM D-1238). All materials were used as received without any modification.

2.2. Preparation of PP/PE blends using ERE

Prior to extrusion, vacuum-dried bulk PP and PE were manually blended with a constant weight ratio of 50/50. The resulting blend was fed into the ERE with a temperature profile from hopper to die of 140–220–220–215 ℃, then extruded at 50 r·min^{-1} through a sheet die with a thickness of 1 mm, and finally cooled in cold water. Specimens for scanning electron microscope (SEM) analysis and mechanical testing were cut along two directions: the machine direction (MD) and the transverse direction (TD).

2.3. Preparation of PP/PE blends using an internal mixer

The reference PP/PE blend was prepared using an internal mixer (MIX) from Brabender (Germany). Following the same procedure as the ERE sample, bulk PP and PE were manually blended with a constant weight ratio of 50/50 and then fed into the internal mixer. Melt compounding was performed at a temperature of 190 °C and a rotor speed of 50 r·min^{-1}. The resulting composite was also cooled in cold water. During fabrication, the time-dependent torque was recorded for reference (Fig. S2 in Appendix A). Samples intended for subsequent SEM characterization and mechanical testing were prepared by compression molding at a pressure of 45 MPa and a temperature of 190 °C.

2.4. Characterizations

The morphological evaluation was conducted using a field-emission SEM (3700 N, Hitachi, Japan) with an applied voltage of 5 kV and a working distance of 13 mm. Prior to evaluation, samples were cryo-fractured after being immersed in a liquid nitrogen bath for at least 30 min and then covered with gold (Au). The size distribution of the resultant PP/PE alloys was analyzed using ImageJ software. For each sample, average values were determined from at least 100 random counts selected from 5–10 SEM images.

PeakForce Quantitative Nanomechanics (QNM) modulus images were obtained by atomic force microscopy (AFM; Dimension FastScan AFM, Bruker, USA) in QNM mode. The microscope was equipped with a tip with a spring contact of 138 N·m^{-1}. The images were analyzed by NanoScope Analysis software (Bruker).

The orientation factor of the ISTSP PP/PE alloy was evaluated using a Fourier-transform infrared (FT-IR) spectrometer (Nicolet Nexus 670, Thermal Scientific, USA) equipped with a polarizer in transmission mode. The evaluation was performed using 64 scans ranging from 400 to 4000 cm^{-1} at a resolution of 8 cm^{-1}. During the evaluation, the direction of the infrared light was adjusted using the polarizer to investigate the orientation of the PP/PE.

Uniaxial tensile tests were conducted using an Instron Universal Tester (5566, Instron, USA) with a load cell of 1 kN at room temperature. A dog-bone-shaped specimen (Fig. S3 in Appendix A) was stretched at a crosshead speed of 20 mm·min^{-1} to realize 100% strain per minute. Strain and stress during the test were recorded for further analysis. These measurements were repeated at least four times to obtain average values.

The dynamic mechanical thermal response of each sample was analyzed using a TA Instruments Dynamic Mechanical Analysis (DMA) Q800 under tensile mode at a frequency of 1 Hz and a temperature ranging from −70 to 100 °C, with a heating rate of 3 °C·min^{-1}. The samples for the test were cut into strips measuring 35 mm × 10 mm × 1 mm (Fig. S3).

Thermogravimetric analysis (TGA) was performed using a Netzsch TG 209 analyzer (Germany) at a temperature from 30 to 600 °C in nitrogen gas to avoid oxidation. The heating rate was 10 °C·min^{-1}. The samples for the test were 6–10 mg.

3. Results and discussion

The morphologies of the as-prepared PP/PE alloys are shown in Figs. 2(a–c). Due to the immiscibility and poor interfacial interaction of these polymers, PP/PE blends usually present a dispersion matrix or co-continuous morphologies, as investigated previously [4,9,10]. The SEM image of the PP/PE that was blended using an internal mixer (MIX) under constant shear flow shows a co-continuous morphology (Fig. 2(a)), in agreement with the theoretical predictions. The SEM image of the ISTSP-produced PP/PE binary blend (named "ISTSP PP/PE") in the TD (Fig. 2(b)) displays a completely different and unusual morphology. Instead of the conventional co-continuous morphology, the ISTSP PP/PE blend exhibits a highly ordered and hexagonal packed structure in the TD, which can be considered a honeycomb structure.

To the best of our knowledge, this is the first report of such a honeycomb morphology being obtained in a PP/PE alloy, or in any other polymeric alloy. In nature, honeybees build a mass of hexagonal prismatic wax cells in their hive. Aside from honeycomb hives, similar honeycomb architectures have been observed in plants [11], the human body [12], and various natural materials [13]. Inspired by this naturally evolved architecture, researchers have found that honeycomb structures exhibit excellent mechanical properties with minimal material density. They also possess several additional functional benefits such as optical properties, electric and thermal conduction, and more [14]. The superior topological advantages of a honeycomb structure have prompted scientists to develop numerous methodologies to fabricate artificial honeycombs from organic and inorganic resources [15]. However, most of the proposed approaches are limited due to their low-efficiency laboratory scale, and normally rely on chemical treatments [16]. In contrast with the state-of-the-art fabrication routes for honeycomb-mimic materials, which can only manufacture several grams at a time, our method produces polymer-based honeycomb structures with a continuous output of over 80 kg·h^{-1} using a 40 mm-diameter rotor, without requiring any additive. We believe that this efficient industry-scale and physical method is much simpler than the existing state-of-the-art routes for the fabrication of honeycomb-structured polymers.

Moreover, we determined that the PP/PE honeycombs display an average wall thickness and cell size of (100 ± 25) and (680 ± 264) nm, respectively (Fig. 2(d)), according to the SEM image shown in Fig. 2(b), which clearly depicts the nanoscale features. Modulus mapping (PeakForce QNM modulus image [17]) of the ISTSP PP/PE blend, as revealed by AFM in the TD, further confirmed the formation of these honeycomb structures (Fig. 2(e)). Moreover, due to the different moduli of PP and PE, modulus mapping was able to distinguish among the honeycomb wall and cell components belonging to the PP and PE phases, respectively.

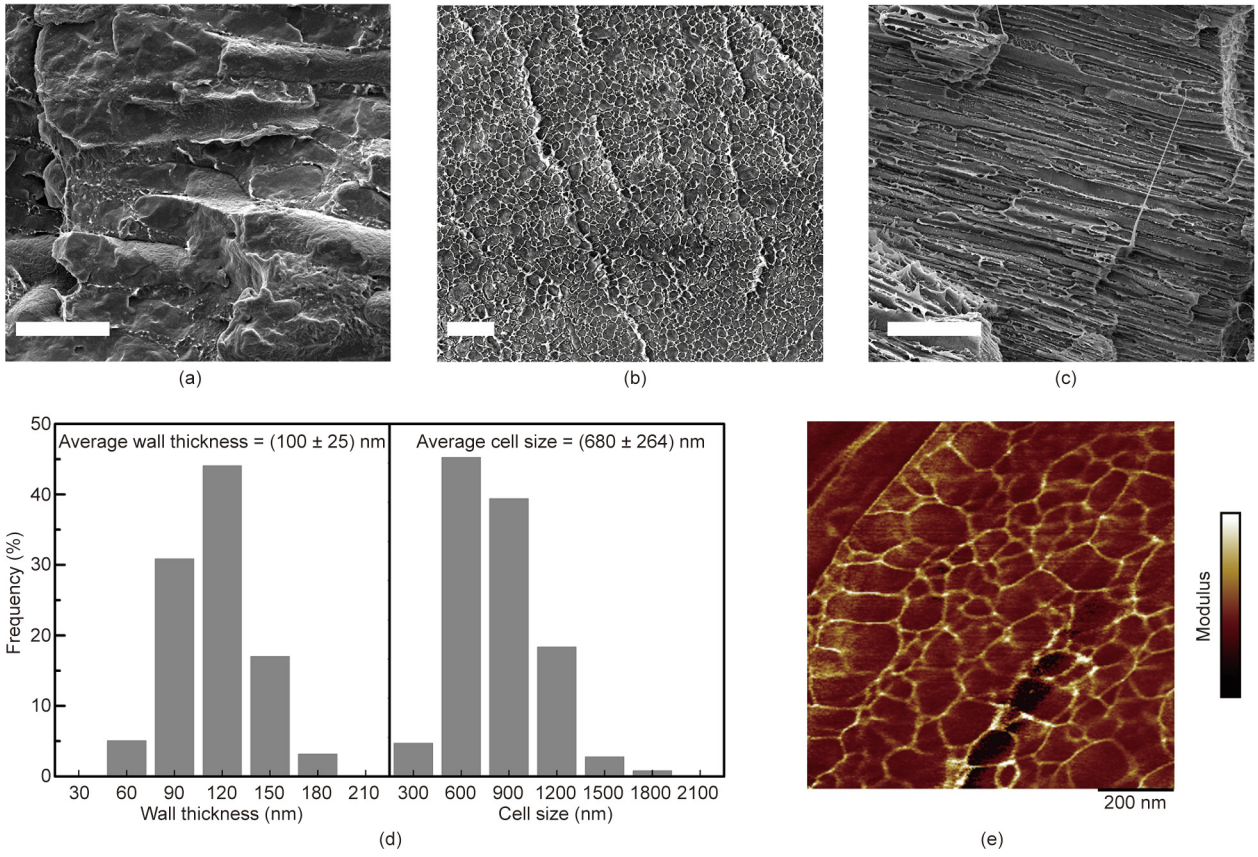

Fig. 2. Morphological characterization of PP/PE alloys blended using MIX and ERE. (a) SEM image in the TD of PP/PE alloy blended using MIX. (b) SEM image in the TD of PP/PE composites blended using the ERE. (c) SEM images in the MD of PP/PE composites blended using the ERE. Scale bars in (a)–(c) are 20 μm. (d) Honeycomb wall and cell size distributions of the ISTSP PP/PE blends measured from the SEM images in the TD. (e) PeakForce QNM modulus images of the ISTSP PP/PE blends in two dimensions to show the honeycomb wall and honeycomb cells belong to the PE and PP phase, respectively.

Next, an analysis of the cryo-fracture surface of the as-prepared sample in the MD was performed, which revealed numerous packed fibrils with a highly ordered orientation (Fig. 2(c)). A polarized FT-IR analysis also showed that the orientation of the PP fibrils is approximately 25% overall and 32% in the crystal phases (for the crystalline information for the PP and PE in the blend (Section S1 and Figs. S4(a,b) in Appendix A), which validates the formation of a highly oriented structure. The orientation of the PE phase in the as-prepared alloy was also confirmed by polarized FT-IR analysis, which revealed different intensities at 920 and 930 cm^{-1} along different polarized angles (Fig. S5 in Appendix A). In addition, the measured length of these fibrils exceeds 100 μm (Fig. 2(c)), which indicates that the length–diameter ratio of the PP/PE honeycombs is greater than 150. To the best of our knowledge, this is the first reported PP/PE alloy presenting such a highly oriented honeycomb nanostructure with such an elevated length–diameter ratio, which can be an essential feature in electric and thermal conduction applications.

The above characterizations indicate that, with the use of ISTSP, we have obtained a PP/PE blend with a novel honeycomb structure via an industrial-scale physical alloying technique. It is necessary to investigate the formation mechanism of such a novel structure. Thus, in Fig. 3, we propose a formation mechanism for the highly oriented nanoscale honeycomb structure under the elongational flow supplied by ISTSP. Fig. 3(a) illustrates how the working process of the rotor in the ERE supplies ISTSP (detailed information can be found in our previous report [18,19]): As shown in the figure, the rotor undergoes a complex movement that combines a constant rotation along its axis with a periodicity altered linear movement in the stator, and consequently generates the elongational flow. Benefiting from the specifically designed working process of the ERE, a cycled transient pressure imitating the ancient process can be realized; the polymeric melts can experience one "elongation–compression" unit (ECU) for each round of rotation, while the microstructures are forced to change.

During the manufacturing by means of ISTSP, we propose that the morphology of the PP/PE alloy evolves in five stages, as repeated ECU cycles occur (Fig. 3(b)). In the first stage, the PP/PE melts exhibit a typical droplet-in-the-sea morphology, with droplets of various shapes being located in the matrix [4]. In this droplet-in-the-sea morphology, the PE is the dispersion phase while the PP is the continuous phase. Upon processing, the combination of elongational flow and thermodynamics drives the shape of the PE droplets to rapidly become spherical and to adopt an island-in-the-sea arrangement (stage 2). Continuous application of the elongational force to the melts transforms the morphology of the PP/PE into stage 3, in which the spherical PE droplets are stretched into rods. After several ECUs have occurred, further stretching causes the PE rods to connect with each other and form a fibrillar morphology (stage 4) [20]. Because the elongational force lies in the MD, the stretch-induced PE fibrils are mostly aligned in this direction. As the melts are continuously pushed toward the die, a growing number of fibrils form and come into contact with each other, eventually reaching stage 5. During extrusion, in combination with the interfacial force between interconnected fibrils and the elongational force along the MD, the PE crystal nucleation and growth transform the PP fibrils into a honeycomb, similar to the formation of a natural honeycomb [16,21].

To test our proposed morphology evolution hypothesis, the microstructures of PP/PE hybrid melts were monitored by examining specimens cut from different positions selected step-by-step along the MD of the ERE (detailed information is included in the Section S2 and Fig. S6 in Appendix A). Fig. 3(c) provides SEM images of PP/PE blends that were selected following the direction of hopper to die, which means that the PP/PE alloy underwent more ECUs than the alloy shown in the SEM images that were

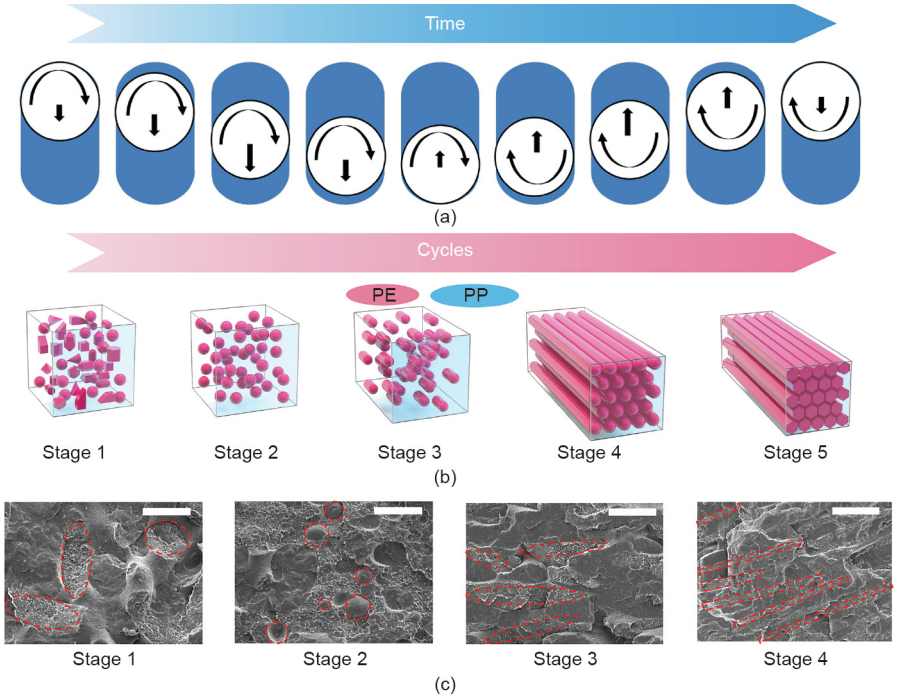

Fig. 3. Morphological evolution of the PP/PE blend melt under elongational flow. (a) Schematic of the rotor movement in the stator in the ERE that can generate elongational flow during processing. (b) The morphology of the sample prepared under elongational flow evolves in five stages: stage 1: droplets-in-the-sea; stage 2: islands-in-the-sea; stage 3: microrods; stage 4: fibrils; stage 5: highly ordered honeycombs. (c) SEM images of PP/PE alloys prepared by ISTSP selected from samples along the rotor, following the direction from hopper to die, showing the following microstructures: droplets-in-the-sea (stage 1), islands-in-the-sea (stage 2), microrods (stage 3), and fibrils (stage 4) (scale bar = 25 μm). Detailed sample selection procedures are provided in the Fig. S3.

taken from left to right. As marked by red dashes, the microstructures that developed—from the droplet-in-the-sea to the fibrillar morphology—provide clear evidence of the transformation from stage 1 to stage 4 described above. Furthermore, it is noticeable that the dispersed phase is randomly located in stages 1 and 2 (Fig. 3(c)), but is highly aligned after more ECUs have occurred (stages 3 and 4). In addition, the honeycomb nanostructure formation mechanism suggests that the intensity of the elongational flow can affect the final morphology of the resultant alloy. To test this possibility, another ERE was specifically designed and built to achieve a weaker elongation flow (for a detailed description, see the Section S2 and Fig. S7 in Appendix A). The resulting sample showed an imperfect microscale honeycomb structure in comparison with the initial ISTSP PP/PE alloy (Fig. 2(b)), thereby highlighting the effect of elongational flow intensity and proving our hypothesis (Fig. S8 in Appendix A). We also monitored the structure of ISTSP PP/PE alloys with different weight ratios and rotation speed, as shown in Fig. S9 in Appendix A, and found that a honeycomb structure can be achieved by means of ISTSP in a wide composition and rotation speed range.

As some of the most important characteristics when a product is evaluated, mechanical properties are essential. Fig. 4 shows the strain–stress curves of the PP/PE alloys prepared using ISTSP and MIX. Given the highly oriented structure, as confirmed in Fig. 1, the mechanical properties of the ISTSP sample are evaluated both in parallel (designated as MD in Fig. 4) and perpendicular (designated as TD in Fig. 4) to the MD. Typically, the tensile strength of a binary blend with ideal dispersion and ideal interfacial adhesion undergoes the rule of mixture. Therefore, according to this rule, the theoretically predicted tensile strength (σ_{rom}) of a PP/PE alloy with a 50/50 weight ratio is 28 MPa (see details in the Section S3 in Appendix A). As has been previously investigated, the tensile properties of PP/PE blends fabricated via conventional techniques commonly follow the rule of mixtures with a negative deviation [2,4].

Because of the poor interfacial adhesion and phase separation, the PP/PE blend prepared using MIX displays a strong negative deviation with σ_{rom} and a brittle fracture prior to or immediately after the yield point. It exhibits a low tensile strength (σ), strain at break (ε), and Young's modulus (E) of 22 MPa, 16%, and 357 MPa, respectively, in agreement with the report by Eagan et al. [2]. In addition, another control sample that was fabricated using a conventional twin-screw extruder was employed and tested, revealing similar tensile properties (Fig. S10 in Appendix A). The tensile properties of the ISTSP PP/PE alloy along the MD increase dramatically, suppressing the theoretically predicted σ_{rom} with an obvious brittle–ductile transition in the tensile behavior. To be specific, the σ, ε, and E values in the MD are 35 MPa, 56%, and 586 MPa, respectively, which are 1.6, 3.5, and 1.6 times greater than the values obtained for the sample prepared using MIX. This substantial enhancement may result from the synergistic effects of the highly oriented alignment, the honeycomb structure, and nanoscale effects. Interestingly, bulk PP and PE display σ values of 30 and 26 MPa, respectively (Fig. S11 in Appendix A), which suggests that the ISTSP PP/PE alloy exhibits a higher tensile stiffness than its individual components. To the best of our knowledge, this is the first immiscible polymer binary blend with a 50/50 weight ratio that presents a higher tensile strength than its parent components in the bulk. Furthermore, from an industrial point of view, such an enhancement of stiffness of PP/PE blends makes it possible for them to replace traditional metal materials in automobiles, railways, and similar applications.

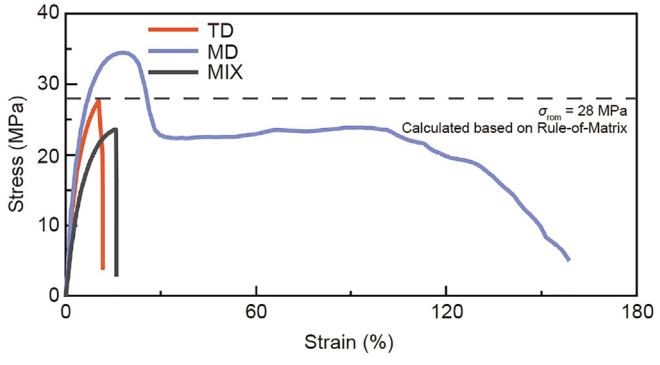

Fig. 4. Mechanical properties of PP/PE alloys blended using MIX and ISTSP. Strain–stress curves of PP/PE blends prepared using MIX and ISTSP in various directions under strain at a rate of 100% per minute (Fig. S9 in Appendix A). The dashed line corresponds to the theoretically predicted tensile strength σ_{rom} of 28 MPa, which is calculated based on the rule of mixtures (for details, see the Section S3 in Appendix A).

To further investigate the highly aligned honeycomb structure, we also tested the tensile properties along the TD. Fig. 4 shows that the formation of the honeycomb nanostructure increases the σ to approximately 28 MPa in the TD, which matches σ_{rom}, while the ISTSP PP/PE alloy still exhibits brittle behavior, similar to its analogue prepared using MIX. The honeycomb structure does not change the tensile fracture behavior of the sample in the TD, but it can make the immiscible PP/PE blend compatible and enhance the blend's strength to achieve the theoretically predicted tensile strength. The tensile strength of the alloy is similar to the rule-of-mixture predicted value, which indicates that the interfacial interaction between PP and PE in the physical structured alloy has been enhanced.

To investigate the reason for this enhancement, we performed a dynamic mechanical analysis (DMA) between the ISTSP-processed sample and the MIX-processed sample (Fig. S12 in Appendix A). The results clearly show that the glass transition temperature (T_g) of the PE in the ISTSP sample is lower than that in the MIX sample, indicating an enhanced mobility of the PE chains in the alloy. Thus, considering such a variation in the T_g and the nanoscale of the PE phase in the ISTSP sample, we can conclude that the PE phase is undergoing nanoconfinement, which has been previously reported to enhance the mobility of macromolecular chains and improve the compatibility of immiscible composites [22,23]. Therefore, we believe that confinement-induced compatibilization is the main contributor to the reinforcement in TD. Moreover, to date, this is the first report realizing such confinement in a polymer/polymer alloy through simple extrusion.

In general, for a given material, an increase in stiffness always comes with a decline in toughness, which makes the balance of these conflicting properties a long-term challenge in material design and fabrication [24,25]. In this study, the ISTSP PP/PE blend simultaneously exhibits improved toughness and enhanced tensile strength. Its work of fracture in the MD (1210 MJ·m^{-3}) is 4.6 times greater than that of the sample prepared using MIX. This superiority in strength and toughness highlights the advantages of the unique honeycomb nanostructure that was obtained during the extrusion. Moreover, the ERE-extruded PP/PE binary blend displays enhanced thermal stability, which can be attributed to the honeycomb structure (Fig. S13 in Appendix A).

4. Conclusions

In summary, with the aim of providing an environmentally friendly way of reusing recycled PP and PE, we employed ISTSP to produce a PP/PE alloy with a novel, highly oriented honeycomb nanostructure by means of an in-house-developed ERE. The ISTSP PP/PE alloy exhibits a brittle–ductile transition and enhanced tensile properties compared with its analogue prepared using MIX. Thanks to the synergistic effects of the highly oriented alignment,

honeycomb architecture, and nanoconfinement effect, the tensile strength of the ISTSP PP/PE alloy exceeds those of its parent components. We believe that our approach can significantly facilitate the development of immiscible polymeric alloys. To further expand our contribution to the specific field of waste plastics remanufacturing, this method can be used to directly reuse a mixture of PP and PE without sorting or using additives. Thus, our findings indicate that ISTSP could be employed for high-performance industry-scale environmentally friendly waste plastics remanufacturing without requiring sorting or the addition of compatibilizers. We also believe that these industrial-scale fabricated nanoscale honeycombs can attract interest from investigators with various backgrounds ranging from optical applications and electric and thermal conduction to drug delivery.

Acknowledgments

We acknowledge the National Key Research and Development Program of China (2019YFC1908202), the Key Program of National Natural Science Foundation of China (51435005), the National Natural Science Foundation of China (51403068), and the China Postdoctoral Science Foundation (2019M652883) for the financial support of this work. Specific acknowledgment is given to the Guangdong Siiico Technology Co., Ltd. for their assistance during the manufacturing of ERE. The authors would also thank Weihua Cheng, Jihai Wu, Xinliang Zou, and Yu Chen for their assistance in this experiment.

Authors' contributions

Jinping Qu, Zhaoxia Huang, and Zhitao Yang devised the original concept and cowrote the manuscript. Zhaoxia Huang fabricated the samples and performed the characterizations. Jinping Qu, Zhaoxia Huang, Zhitao Yang, Guizhen Zhang, and Xiaochun Yin designed the ERE used in this work. Zhaoxia Huang, Hezhi He, and Yanhong Feng analyzed the SEM data. Gang Jin helped the tensile tests. Ting Wu, Guangjian He, and Xianwu Cao were responsible for the FT-IR and AFM results. All authors proofread and commented this manuscript.

Compliance with ethics guidelines

Jinping Qu, Zhaoxia Huang, Zhitao Yang, Guizhen Zhang, Xiaochun Yin, Yanhong Feng, Hezhi He, Gang Jin, Ting Wu, Guangjian He, and Xianwu Cao declare that they have no conflict of interest or financial conflicts to disclose.

Appendix A. Supplementary data

Supplementary data to this article can be found online at https://doi.org/10.1016/j.eng.2021.02.021.

References

[1] Geyer R, Jambeck JR, Law KL. Production, use, and fate of all plastics ever made. Sci Adv 2017;3(7):e1700782.
[2] Eagan JM, Xu J, Di Girolamo R, Thurber CM, Macosko CW, LaPointe AM, et al. Combining polyethylene and polypropylene: enhanced performance with PE/*i*PP multiblock polymers. Science 2017;355(6327):814–6.
[3] Meran C, Ozturk O, Yuksel M. Examination of the possibility of recycling and utilizing recycled polyethylene and polypropylene. Mater Des 2008;29(3):701–5.
[4] Teh JW, Rudin A, Keung JC. A review of polyethylene–polypropylene blends and their compatibilization. Adv Polym Technol 1994;13(1):1–23.
[5] Rahimi A, García JM. Chemical recycling of waste plastics for new materials production. Nat Rev Chem 2017;1(6):1–11.
[6] Pivnenko K, Eriksen MK, Martín-Fernández JA, Eriksson E, Astrup TF. Recycling of plastic waste: presence of phthalates in plastics from households and industry. Waste Manage 2016;54:44–52.
[7] Zhao Y, Lv X, Ni H. Solvent-based separation and recycling of waste plastics: a review. Chemosphere 2018;209:707–20.
[8] Song, Y. T'ien-Kung K'ai-Wu: Chinese technology in the seventeenth century. University Park: Pennsylvania State University Press; 1966.
[9] Noel III OF, Carley JF. Morphology of polyethylene–polypropylene blends. Polym Eng Sci 1984;24(7):488–92.
[10] Tripathi SN, Rao GSS, Mathur AB, Jasra R. Polyolefin/graphene nanocomposites: a review. RSC Adv 2017;7(38):23615–32.
[11] Gibson LJ. The hierarchical structure and mechanics of plant materials. J R Soc Interfaces 2012;9(76):2749–66.
[12] Nedjari S, Awaja F, Altankov G. Three dimensional honeycomb patterned fibrinogen based nanofibers induce substantial osteogenic response of mesenchymal stem cells. Sci Rep 2017;7:15947.
[13] Xiong W, Gao Y, Wu Xu, Hu X, Lan D, Chen Y, et al. Composite of macroporous carbon with honeycomb-like structure from mollusc shell and $NiCo_2O_4$ nanowires for high-performance supercapacitor. ACS Appl Mater Interf 2014;6(21):19416–23.
[14] Wahl L, Maas S, Waldmann D, Zürbes A, Frères P. Shear stresses in honeycomb sandwich plates: analytical solution, finite element method and experimental verification. J Sandw Struct Mater 2012;14(4):449–68.
[15] Zuo D, Zhang L, Yi C, Zuo H. Effects of compatibility of poly(*L*-lactic-acid) and thermoplastic polyurethane on mechanical property of blend fiber. Polym Adv Technol 2015;25(12):1406–11.
[16] Chisca S, Musteata VE, Sougrat R, Behzad AR, Nunes SP. Artificial 3D hierarchical and isotropic porous polymeric materials. Sci Adv 2018;4(5):eaat0713.
[17] Pittenger B, Erina N, Su C. Quantitative mechanical property mapping at the nanoscale with PeakForce QNM. Report. Santa Barbara: Bruker Nano Surfaces Division; 2010.
[18] Zhang G, Wu T, Lin W, Tan Y, Chen R, Huang Z, et al. Preparation of polymer/clay nanocomposites via melt intercalation under continuous elongation flow. Compos Sci Technol 2017;145:157–64.
[19] Qu J, Zhang G, Yin X, inventors; South China University of Technology, Guangzhou Huaxinke Enterprise Co., assignees. Volume pulsed deformation plasticating and conveying method and device by eccentric rotor. United States patent US 20170080619. 2017 Mar 23.
[20] Zhou S, Huang H, Ji X, Yan D, Zhong G, Hsiao BS, et al. Super-robust polylactide barrier films by building densely oriented lamellae incorporated with ductile in situ nanofibrils of poly (butylene adipate-*co*-terephthalate). ACS Appl Mater Interfaces 2016;8(12):8096–109.
[21] Thompson DW. On growth and form. New York: Dover Publications; 1942.
[22] Shin K, Obukhov S, Chen JT, Huh J, Hwang Y, Mok S, et al. Enhanced mobility of confined polymers. Nat Mater 2007;6(12):961–5.
[23] Rittigstein P, Priestley RD, Broadbelt LJ, Torkelson JM. Model polymer nanocomposites provide an understanding of confinement effects in real nanocomposites. Nat Mater 2007;6(4):278–82.
[24] Ritchie RO. The conflicts between strength and toughness. Nat Mater 2011;10(11):817–22.
[25] Wang Y, Chen M, Zhou F, Ma En. High tensile ductility in a nanostructured metal. Nature 2002;419(6910):912–5.